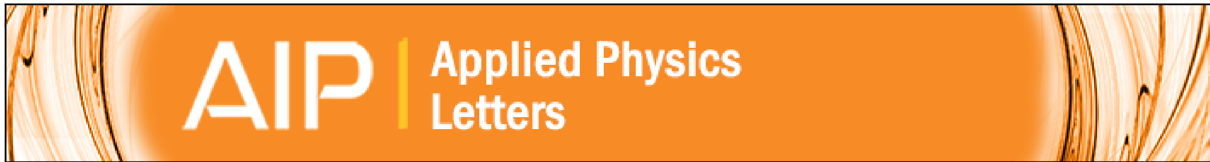


# High-resolution depth profiling in ultrathin $Al_2O_3$ films on Si

E. P. Gusev, M. Copel, E. Cartier, I. J. R. Baumvol, C. Krug, and M. A. Gribelyuk

Citation: Applied Physics Letters **76**, 176 (2000); doi: 10.1063/1.125694
View online: http://dx.doi.org/10.1063/1.125694
View Table of Contents: http://scitation.aip.org/content/aip/journal/apl/76/2?ver=pdfcov
Published by the AIP Publishing

**Articles you may be interested in**

High resolution medium energy ion scattering analysis for the quantitative depth profiling of ultrathin high- k layers
J. Vac. Sci. Technol. B **28**, C1C65 (2010); 10.1116/1.3248264

Atomic layer deposition of $Al_2O_3$ thin films using dimethylaluminum isopropoxide and water
J. Vac. Sci. Technol. A **21**, 1366 (2003); 10.1116/1.1562184

Investigation of the effect of high-temperature annealing on stability of ultrathin $Al_2O_3$ films on Si(001)
J. Appl. Phys. **92**, 1914 (2002); 10.1063/1.1495066

Ultrathin nitrided-nanolaminate ( $Al_2O_3$ / $ZrO_2$ / $Al_2O_3$ ) for metal–oxide–semiconductor gate dielectric applications
J. Vac. Sci. Technol. B **20**, 1143 (2002); 10.1116/1.1481864

Robustness of ultrathin aluminum oxide dielectrics on Si(001)
Appl. Phys. Lett. **78**, 2670 (2001); 10.1063/1.1367902

NEW Special Topic Sections
NOW ONLINE
Lithium Niobate Properties and Applications: Reviews of Emerging Trends
AIP Applied Physics Reviews

Reuse of AIP Publishing content is subject to the terms at: https://publishing.aip.org/authors/rights-and-permissions. Download to IP: 143.54.44.137 On: Thu, 05 May 2016 16:32:09

APPLIED PHYSICS LETTERS VOLUME 76, NUMBER 2 10 JANUARY 2000

# High-resolution depth profiling in ultrathin $Al_2O_3$ films on Si

E. P. Gusev,[a] M. Copel, and E. Cartier
*IBM T. J. Watson Research Center, Yorktown Heights, New York 10598*

I. J. R. Baumvol and C. Krug
*Instituto de Física, UFRGS, Porto Alegre, RS, Brazil 91509-900*

M. A. Gribelyuk
*IBM Analytical Services, Hopewell Junction, New York 12533*

(Received 20 September 1999; accepted for publication 10 November 1999)

A combination of two complementary depth profiling techniques with sub-nm depth resolution, nuclear resonance profiling and medium energy ion scattering, and cross-sectional high-resolution transmission electron microscopy were used to study compositional and microstructural aspects of ultrathin (sub-10 nm) $Al_2O_3$ films on silicon. All three techniques demonstrate uniform continuous films of stoichiometric $Al_2O_3$ with abrupt interfaces. These film properties lead to the ability of making metal-oxide semiconductor devices with $Al_2O_3$ gate dielectric with equivalent electrical thickness in the sub-2 nm range. © *2000 American Institute of Physics.* [S0003-6951(00)02402-5]

Aggressive shrinking of the thickness of $SiO_2$-based gate dielectrics in logic and memory semiconductor devices below $\sim 2-3$ nm brings about a number of fundamental problems for further oxide scaling, with the most critical ones being reduced dielectric reliability and exponentially increasing leakage (tunneling) current with decreasing oxide thickness.[1,2] This dictates a search for alternative materials with a dielectric constant higher than that of $SiO_2$ ($\epsilon_{SiO_2} = 3.8$). Aluminum oxide ($Al_2O_3$) and other alumina-based materials are considered to be candidates for gate dielectric applications.[1–3] An attractive feature of this material is that, in contrast to most high-K materials for which higher dielectric constant usually comes at the expense of narrower band gap[4] (and consequently lower barrier height for electrons and holes which determines leakage current), $Al_2O_3$ has the band gap similar to $SiO_2$ and the dielectric constant more than twice higher ($\epsilon_{Al_2O_3} \sim 9$, for thin films). It is not surprising therefore to find reports on thick $Al_2O_3$ gate oxides in metal-oxide semiconductor (MOS) devices in the beginning of the integrated circuit history.[5–7] However, the properties of ultrathin $Al_2O_3$ films and processing and integration issues behind their use for future deep sub-$\mu$m MOS devices are not yet well understood.

For an electrical equivalent oxide thickness (defined as $d_{EOT} = d_{phys}\, \epsilon_{SiO_2}/\epsilon_{Al_2O_3}$) in the sub-2 nm range, the physical thickness ($d_{phys}$) of $Al_2O_3$ layers should be less than approximately 4 nm. For such ultrathin films on silicon substrate, a challenging task is their physical characterization. In this thickness range most profiling techniques do not offer the required sub-nm depth resolution.[8,9] In this letter, we use a combination of powerful methods including a technique of nuclear resonance profiling, NRP [based on a low-energy, very narrow resonance in the cross section curve of the nuclear reaction $^{27}Al(p,\gamma)^{28}Si$], medium energy ion scattering (MEIS) and high-resolution transmission electron microscopy (HRTEM) to physically characterize ultrathin gate-quality $Al_2O_3$ films on Si with sub-nm resolution.

Nuclear resonance profiling (NRP) with the narrow, isolated resonance[10] at 404.9 keV in the cross section curve of the $^{27}Al(p,\gamma)^{28}Si$ nuclear reaction was used to obtain Al concentration depth distributions. The measured excitation curves (i.e., $\gamma$-ray yield versus incident proton energy) around the resonance energy ($E_R$) were converted into concentration profiles using the SPACES program,[11] which is based on the stochastic theory of energy loss of ions in matter. By measuring the excitation curves for thin and thick aluminum films, the nuclear reaction resonance at 404.9 keV was determined to be narrower than 40 eV. A highly tilted sample geometry ($\Psi = 65°$ with respect to the incident beam) was used to increase depth resolution. Several factors contribute to the obtained depth resolution of 0.4–0.5 nm near the surface[12] (i) an extremely narrow nuclear reaction resonance ($\Gamma_R \leqq 40$ eV); (ii) a significant energy loss of 405 keV protons in $Al_2O_3$ (approximately $380\,\mathrm{keV\,mg^{-1}}\,cm^{-2}$, if a density of $3.98\,\mathrm{g\,cm^{-3}}$ is assumed for $Al_2O_3$); (iii) a low energy spread of the proton beam (FWHM $\sim 80$ eV at 405 keV), as provided by the 500 keV HVEE ion implanter in Porto Alegre; and (iv) an apparent thickness magnification by a factor of 2.4 due to the tilted geometry.

In addition to NRP, other powerful analytical techniques, such as MEIS, HRTEM and ellipsometry (both single-wavelength at 635 nm and spectroscopic), were used in this study. MEIS analysis was performed with 200 keV $He^+$ ions as a probe.[8,13,14] A channeling scattering geometry with the ion beam aligned along the $[11\bar{1}]$ axis of Si was used. The scattering angle was 60°. The net depth resolution of MEIS (based on combined energy resolution of the detector and the accelerator) was below 1 nm. The depth profiles were obtained from the simulations assuming stoichiometric $Al_2O_3$ with the density of of $3.98\,\mathrm{g/cm^3}$ (same as in the NRP) and the stopping power of 200 keV $He^+$ ions in $Al_2O_3$ of $1060\,\mathrm{keV\,mg^{-1}}\,cm^{-2}$. More details about the MEIS setup and depth profiling analysis can be found elsewhere.[8,9,13,14] Cross-sectional images of selected samples were obtained by high resolution transmission electron microscopy (HRTEM)

[a]Electronic mail: gusev@us.ibm.com

Reuse of AIP Publishing content is subject to the terms at: https://publishing.aip.org/authors/rights-and-permissions. Download to IP: 143.54.44.137 On: Thu, 05 May 2016 16:32:09

 © 2000 American Institute of Physics

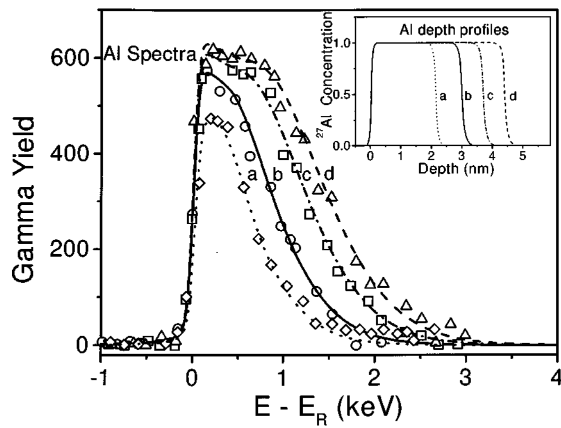


FIG. 1. Excitation curves of the $^{27}Al(p,\gamma)^{28}Si$ nuclear reaction around the resonance at 404.9 keV for ultrathin $Al_2O_3$ films deposited on underlaying $SiO_xN_y$ (a) or $SiO_2$ (b), (c), and (d) films. The lines represent simulations of the experimental excitation curves with the program SPACES. The inset shows the $^{27}Al$ vs depth distributions (normalized to $Al_2O_3$) used for the simulation of each of the excitation curves.

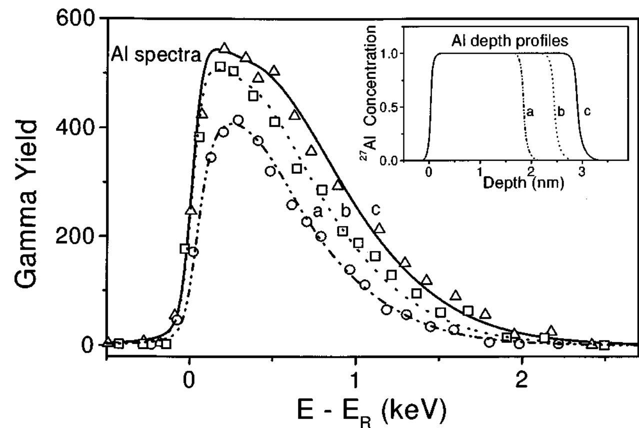


FIG. 2. Excitation curves and the corresponding simulations (lines) for the $^{27}Al(p,\gamma)^{28}Si$ nuclear reaction around the resonance at 404.9 keV for aluminum oxide films with increasing thickness deposited on Si(001) substrates cleaned in a diluted HF. The $^{27}Al$ vs depth distributions (normalized to $Al_2O_3$) used for the simulation of each of the excitation curves are shown in the inset.

in an HF-2000 electron microscope operated at 200 kV accelerating voltage which offers a point-to-point spatial resolution of $\sim 0.24$ nm.

Ultrathin (2–8 nm) films of $Al_2O_3$ were deposited on Si(100) ($p$ and $n$ type) wafers by atomic layer chemical vapor deposition (ALCVD) using a Microchemistry F-200 reactor. Cycles of trimethylaluminum (TMA) and water were used to grow the films.[15] Prior to the deposition, the wafers received a standard chemical preclean followed by thermal oxidation to grow an ultrathin ($\sim 1-1.5$ nm) oxide or oxynitride. To understand the quality of the $Al_2O_3$/Si interface, some of the wafers were treated in diluted HF immediately before deposition to make H-passivated surface.

Excitation curves of the $^{27}Al(p,\gamma)^{28}Si$ nuclear reaction around the resonance at 404.9 keV are shown in Fig. 1 for aluminum oxide films deposited on a thin silicon oxide thermally grown on Si(001). The distinct separation of the spectra for the films differing by only 1–2 nm demonstrates the high (sub-nm) depth resolution of the technique. The lines through the experimental points are a result of the simulation obtained with the help of SPACES for the Al profiles shown in the inset. The $^{27}Al$ concentrations are given with respect to $Al_2O_3$. One can clearly see the aluminum concentration in the films is constant (within the depth resolution of the technique), equal to the aluminum concentration in stoichiometric $Al_2O_3$. The conclusion on $Al_2O_3$ stoichiometry was confirmed by comparing the excitation curves of ultrathin films in question with those of thick $Al_2O_3$ standards. One should also note an abrupt interface with the underlying silicon oxide.

For $Al_2O_3$ films deposited on Si right after HF treatment, excitation curves, and corresponding depth profiles (Fig. 2) look very similar to the case of the deposition on ultrathin thermal $SiO_2$ films (Fig. 1). Here again, one should stress: (i) uniform films with constant concentration of Al through the films, and (ii) sharp interfaces.

MEIS spectra of $Al_2O_3$ films on thermally grown oxynitride and HF-cleaned surface are shown in Figs. 3(a) and 3(b), as well as the results of spectral deconvolution into the oxygen, aluminum, and silicon components. A small nitrogen peak is also seen in the sample with the oxynitride underlayer. Complementary to NRP, MEIS allows for oxygen (and silicon) profiling in addition to the aluminum depth distributions. The simulation of the spectra yielded the following results. For the $Al_2O_3/SiO_xN_y$/Si sample, the best fit was obtained in a model of $\sim 2.0 \pm 0.3$ nm of an $Al_2O_3$ layer on $\sim 0.5 \pm 0.3$ nm bottom oxynitride. For the H-passivated sample, the simulations resulted in a $\sim 2.4 \pm 0.3$ nm $Al_2O_3$ layer without an interfacial oxide. In both cases MEIS results are supportive of stoichiometric $Al_2O_3$ films with abrupt interfaces.

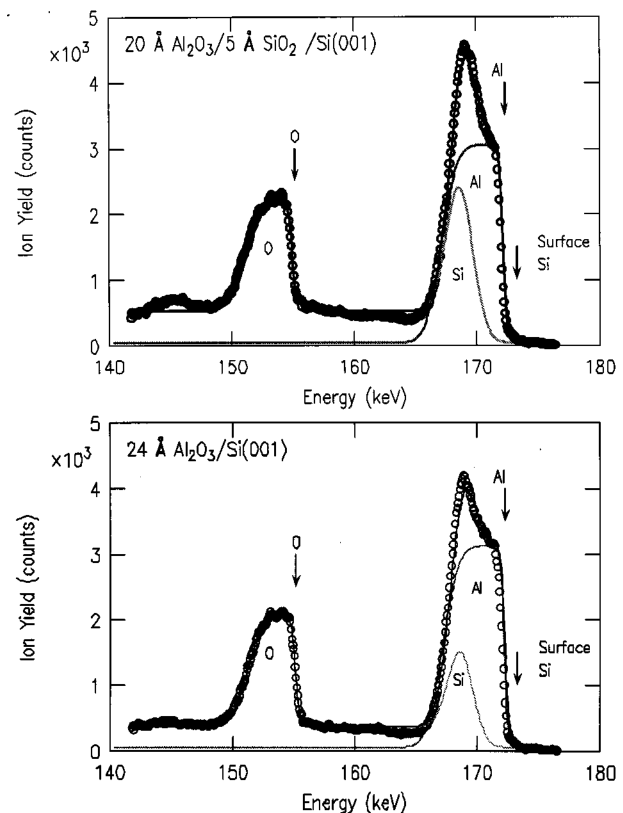


FIG. 3. MEIS spectra of an $\sim 3$ nm $Al_2O_3$ film deposited on ultrathin $SiO_xN_y$ (a) and HF-treated Si (b). The spectra are deconvolved into Si and Al contributions.

Reuse of AIP Publishing content is subject to the terms at: https://publishing.aip.org/authors/rights-and-permissions. Download to IP: 143.54.44.137 On: Thu, 05 May 2016 16:32:09

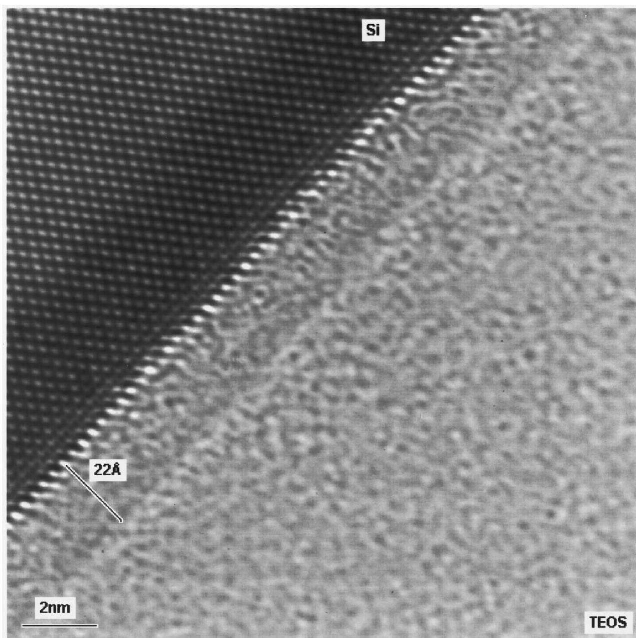


FIG. 4. Cross-sectional HRTEM of an $Al_2O_3$ film deposited on HF-treated Si, MEIS spectrum of which is shown in Fig. 3b.

Complementary to the above ion beam techniques, powerful for the compositional analysis, HRTEM was employed to explore microstructural aspects of the films in question (Fig. 4). A uniform continuous film is observed. The as-deposited films are amorphous. For the HF treated sample, the present analysis shows no evidence for interfacial $SiO_x$ layer (although one should keep in mind that the atomic scattering amplitudes for electrons of Al and Si are very close which may result in poor TEM contrast difference between $Al_2O_3$ and $SiO_x$). Physical thickness of the $Al_2O_3$ layer is deduced to be $2.2\pm0.3$ nm, in good agreement with the NRP and MEIS results.

All three techniques yield similar results that can be summarized as follows. Ultrathin $Al_2O_3$ films deposited on Si (or on the bottom oxide or oxynitride layer) by the ALCVD technique show: (i) good uniformity; (ii) $Al_2O_3$ stoichiometry; and (iii) abrupt interfaces. These results imply the films should have good electrical properties. In fact, our electrical measurements (Fig. 5) support this statement. The quasistatic capacitance–voltage (C–V) measurements indicate a small dc leakage for the larger voltages. By changing the ramp rate, we have verified that this leakage does not distort the quasistatic C–V in the relevant interval $[-1,0]$. As can be seen, the interface state density is low. The high frequence C–V was ramped from $-2$ V to $+2$ V and back. Very little hysteresis is observed in this voltage range. Scanning to larger voltages indicated the occurrence of some electron trapping, evidenced by a flatband shift towards more positive voltages.

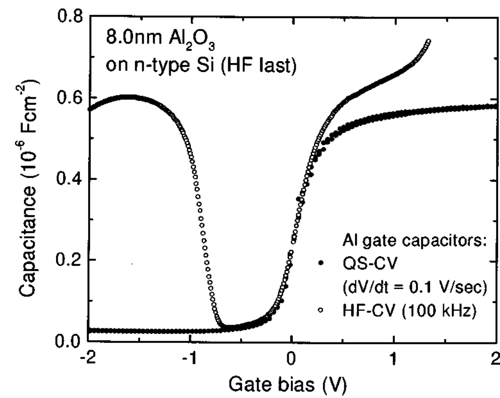


FIG. 5. Quasistatic (open symbols) and high-frequency (solid symbols) capacitance–voltage curves measured on an Al gate capacitor with an annealed film of $Al_2O_3$ dielectric with the physical thickness of ~8.0 nm.

The authors would like to thank J. Skarp, S. Haukka, M. Tuominen, M. Jussila, of AFM Microchemistry Ltd. for their help with deposition; C. D'Emic for the growth of high-quality ultrathin thermal oxides and oxynitrides; and D. Buchanan, S. Guha, and H. Okorn-Schmidt for discussions.

[1] D. Buchanan, IBM J. Res. Dev. **43**, 245 (1999).
[2] L. Feldman, E. P. Gusev, and E. Garfunkel, in *Fundamental Aspects of Ultrathin Dielectrics on Si-based Devices*, edited by E. Garfunkel, E. P. Gusev, and A. Y. Vul' (Kluwer Academic, Dordrecht, 1998), p. 1.
[3] L. Manchanda, W. H. Lee, J. E. Bower, F. H. Baumann, W. L. Brown, C. J. Case, R. C. Keller, Y. O. Kim, E. J. Laskowski, M. D. Morris, R. L. Opila, P. J. Silverman, T. W. Sorsch, and G. R. Weber, Tech. Dig. Int. Electron Devices Meet. **1998**, 605 (1998).
[4] S. A. Campbell, D. C. Gilmer, X. C. Wang, M. T. Hsieh, H. S. Kim, W. Gladfelter, and J. Yan, IEEE Trans. Electron Devices **44**, 104 (1997).
[5] J. A. Aboaf, J. Electrochem. Soc. **114**, 948 (1967).
[6] M. T. Duffy and A. G. Revesz, J. Electrochem. Soc. **117**, 372 (1970).
[7] M. T. Duffy and W. Kern, RCA Rev. **31**, 754 (1970).
[8] E. P. Gusev, H. C. Lu, E. Garfunkel, T. Gustafsson, and M. Green, IBM J. Res. Dev. **43**, 265 (1999).
[9] A. C. Diebold, D. Venables, Y. Chabal, D. Muller, M. Weldon, and E. Garfunkel, Mater. Sci. Semicond. Process. **2**, 103 (1999).
[10] S. E. Hunt and W. M. Jones, Phys. Rev. **89**, 1283 (1953).
[11] I. Vickridge and G. Amsel, Nucl. Instrum. Methods Phys. Res. B **45**, 6 (1990).
[12] G. Battistig, G. Amsel, I. Trimaille, J.-J. Ganem, S. Rigo, F. C. Stedile, I. J. R. Baumvol, W. H. Schulte, and H. W. Becker, Nucl. Instrum. Methods Phys. Res. B **85**, 326 (1993).
[13] J. F. van der Veen, Surf. Sci. Rep. **5**, 199 (1985).
[14] R. M. Tromp, M. Copel, M. C. Reuter, M. Horn von Hoegen, J. Speidell, and R. Koudijs, Rev. Sci. Instrum. **62**, 2679 (1991).
[15] P. Ericsson, S. Bengtsson, and J. Skarp, Microelectron. Eng. **36**, 91 (1997).

Reuse of AIP Publishing content is subject to the terms at: https://publishing.aip.org/authors/rights-and-permissions. Download to IP: 143.54.44.137 On: Thu, 05 May 2016 16:32:09